JOURNAL OF MATERIALS SCIENCE 27 (1992) 1197–1201

Optical properties of Bi_2Te_2Se thin films

E. Kh. SHOKR, M. M. WAKKAD
Physics Department, Faculty of Science, Sohag, Egypt

Some optical parameters of Bi_2Te_2Se thin films, determined from the measured absorbance and transmittance at normal incidence in the visible spectral range, were studied as functions of film thickness and annealing temperature. These parameters were found to be sensitive to both film thickness and microstructure change caused by annealing in a film. The effect of thickness and temperature of annealing on the optical gap was interpreted in terms of elimination of defects and change of disordering in the amorphous matrix.

1. Introduction

Nowadays, interest in solar absorption has created a great demand for studies of the optical absorption spectra and determination of the optical constants of actual thin films of absorbing semiconductor materials in the visible and infrared spectrum regions. Chalcogenides are promising as solar cell materials due to the advantage of easy film formation inherent to the glasses.

It has been shown by many workers that the electrical properties of semiconductors are strongly dependent upon the band gap [1, 2]. Glassy chalcogenide semiconductors show great variations in band gap values, which is influenced by the variation in the composition of such materials (e.g. [3–5]). Studies on the infrared absorption for Bi_2TeSe_2 and Bi_2Te_2Se compounds [6] showed that both compounds seemed to be narrow band gap semiconductors with optical gap values of 0.1 and 0.075 eV, respectively. The difference in band gap ($E_g = 0.025$ eV) was attributed to the increase in the percentage of tellurium which creates localized states in the band gap because of the local perturbation of the structure. In addition, it has been reported that excess tellurium and the Se–Te system continuously decrease the activation energy with increasing percentage of tellurium [7]. The increase in the number of tellurium atoms can reflect the decrease in band gap [2]. However, studies on the optical properties of Bi_2Te_2Se thin films in the visible spectral range have not received any attention.

On the other hand, variations in the optical properties of Bi_2Te_2Se alloy with thickness and heat treatment of the films deserves a comprehensive investigation. As extrapolation [8–10] changing of either film thickness or heat treatment is expected to be associated with corresponding changes in the number of disorders and defects in the amorphous structure of chalcogenide materials. Thus, it was decided to study the effect of both film thickness and microstructure change caused by annealing on some of the optical parameters of Bi_2Te_2Se thin films in the spectral range 380–780 nm.

2. Experimental procedure

Bulk material of Bi_2Te_2Se alloy was prepared from 99.999% pure bismuth, tellurium and selenium by means of the usual melt–quench technique, as described elsewhere [11]. In addition, quenching was performed at 0 °C in ice–water. The microstructure analysis was performed using an X-ray diffractometer type Philips model PW1710. The powder X-ray diffractogram shown in Fig. 1 proved that the structure of the as-prepared ingot consists of polycrystalline Bi_2Te_2Se phase [6].

Thin films of the prepared composition were deposited at room temperature at a deposition rate of 2 nm s^{-1}, by thermal evaporation under a vacuum of 5×10^{-5} torr (1 torr = 1.333×10^2 Pa) using an Edward's high-vacuum coating unit model E306A. Clean Corning glass was used as substrates. The thickness of a film was controlled by means of an Edward's high-vacuum FTM5 film thickness monitor.

Both absorbance, A, and transmittance, T, of a film were measured by using a Cecil CE599 double-beam automatic scanning spectrophotometer combined with a CE836 program controller in the spectral range 380–780 nm at normal incidence. The spectral dependence of both A and T for virgin and annealed films with film thickness, d (nm), and temperature of annealing, T_a (°C), were as shown in Figs 2 and 3, respectively.

Annealing was carried out at a particular temperature for 12 min. The proposed parameters were measured after cooling films to room temperature.

3. Results and discussion

3.1. X-ray diffraction analysis

Considering the X-ray diffractograms shown in Figs 1 and 4, the following general features can be extracted. The method used for preparation of the working material resulted in good alloying, because X-ray peaks corresponding to elemental or binary constituents are not included. The prepared films were

0022–2461

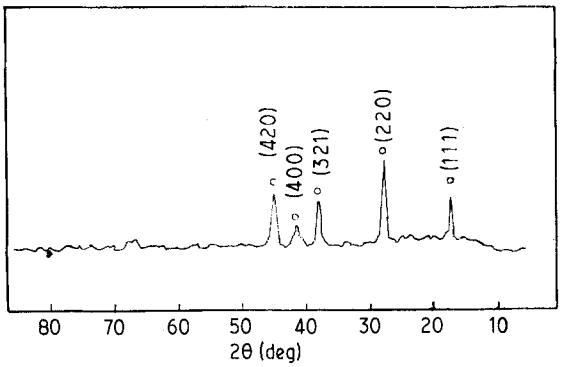

Figure 1 X-ray diffraction pattern for the as-prepared ingot. (○) Bi_2Te_2Se.

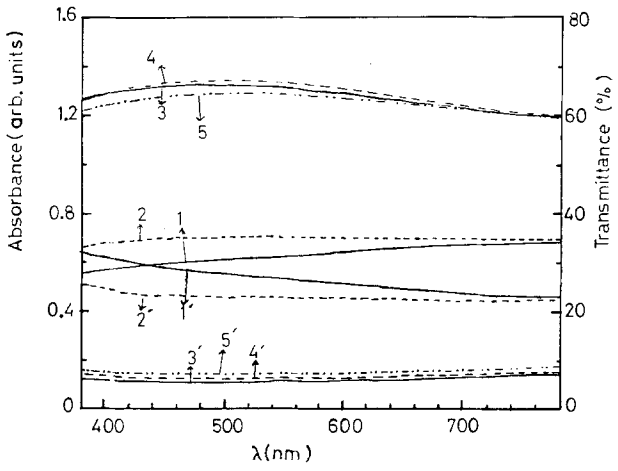

Figure 2 Spectral dependence of (1–5) absorbance and (1′–5′) transmittance for as-deposited films prepared at (1, 1′) 80, (2, 2′) 100, (3, 3′) 120, (4, 4′) 150, (5, 5′) 200 nm film thickness.

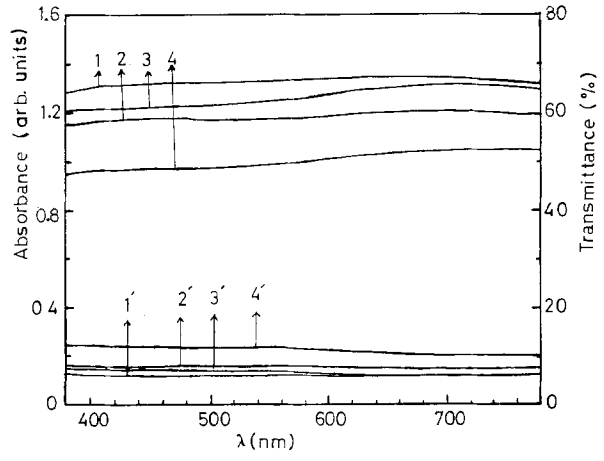

Figure 3 Spectral dependence of (1–4) absorbance and (1′–4′) transmittance for films annealed at T_a (°C) = (1, 1′) 200, (2, 2′) 250, (3, 3′) 350 and (4, 4′) 400 for 12 min. d = 120 nm.

polycrystalline which are embedded in an amorphous matrix. The degree of disordering changes nonsequentially in a film with increasing annealing temperature, as can be confirmed from the nonsequential revelation and nonsequential intensity change of X-ray peaks with T_a. However, the observed decrease in the intensity of peaks at T_a = 400 °C may be caused by the loss of metallic tellurium atoms as $T_a \geqslant 375$ °C [12].

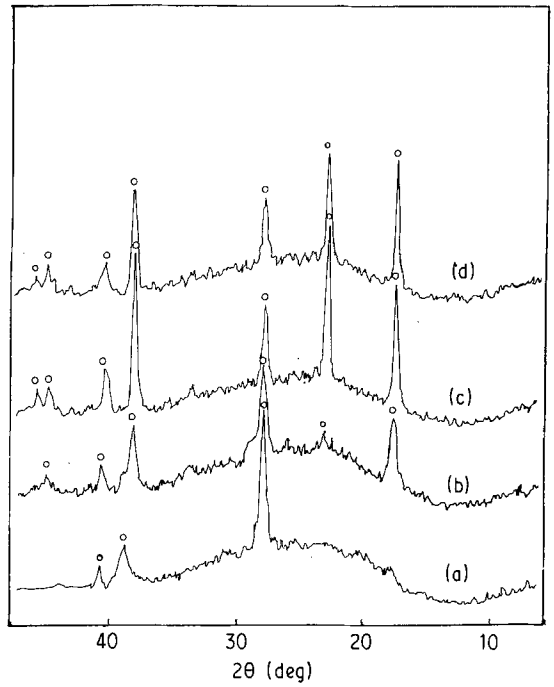

Figure 4 X-ray diffraction spectra of (○) Bi_2Te_2Se thin films: (a) as-deposited film, and (b–d) films heat-treated at 250, 350 and 400 °C for 12 min, respectively.

3.2. Optical gap, E_{opt}

For many glassy and amorphous non-metallic materials, the absorption edge can be divided into two regions depending on the value of the absorption coefficient, α. For $\alpha < 10^4\ cm^{-1}$ there is usually an Urbach tail [13] in which α depends exponentially on photon energy, $h\nu$. Accordingly [14, 15] for $10^4 \leqslant \alpha\ (cm^{-1}) \leqslant 10^6$ the following relation is obeyed

$$\alpha h\nu = B(h\nu - E_{opt})^r \quad (1)$$

where $h\nu$ is the incident photon energy, B is a parameter that depends on the transition probability and r is a number which characterizes the transition process. The usual method for the determination of the values of E_{opt} and B involves plotting a graph of $(\alpha h\nu)^{1/r}$ against $h\nu$.

An analysis of the spectra of Figs 2 and 3 shows that α is in the high absorption region because it takes values in the range 5.2×10^4–$11.4 \times 10^4\ cm^{-1}$. In addition, the spectral variation in α for either virgin or annealed specimens can be described by Equation 1 with $r = \frac{1}{2}$, indicating direct allowed transitions in the ranges of $h\nu$ of approximately 2–3 and 2.21–3.16 eV, respectively (Figs 5 and 6). The determined values of E_{opt} and B are listed in Table I. As shown, the optical gap increases from ~ 0.66 eV reaching its saturation value ~ 1.21 eV with increasing film thickness from 80–150 nm. This effect of film thickness on E_{opt} can be interpreted, as for a-$In_{0.4}Se_{0.6}$ films [8], in terms of the elimination of defects in the amorphous structure. The insufficient number of atoms deposited in the amorphous film results in the existence of unsaturated bonds. These bonds are responsible for the formation of some defects in the films which produce localized states in the band gap. Thicker films are characterized by a homogeneous network, which minimizes the number

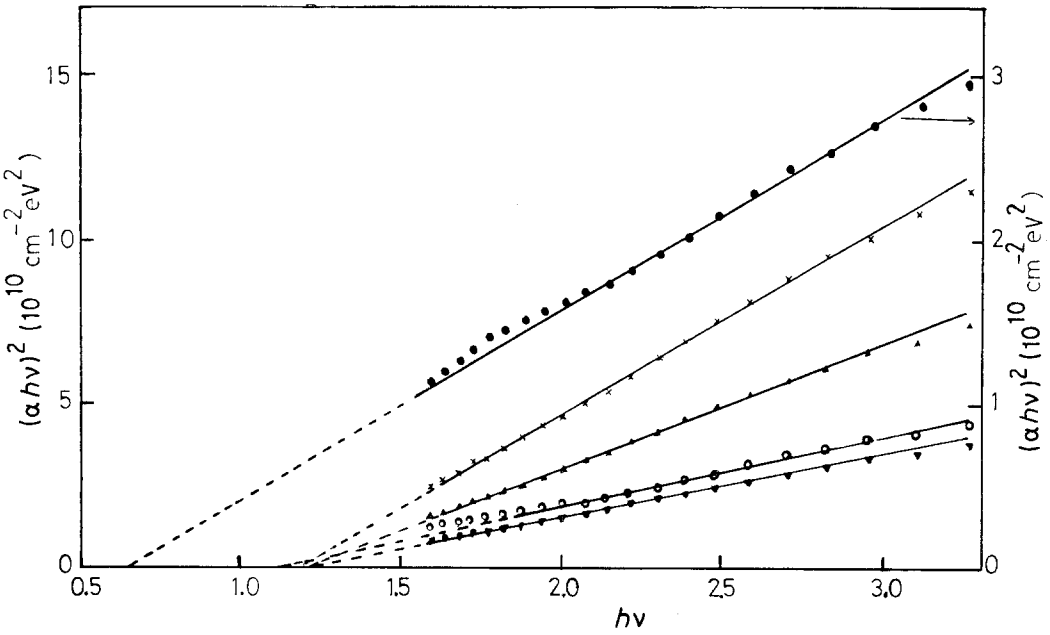

Figure 5 $(\alpha h\nu)^2$ versus $h\nu$ for as-deposited films at d (nm) = (●) 80, (○) 100, (×) 120, (▲) 150, and (▼) 200 nm.

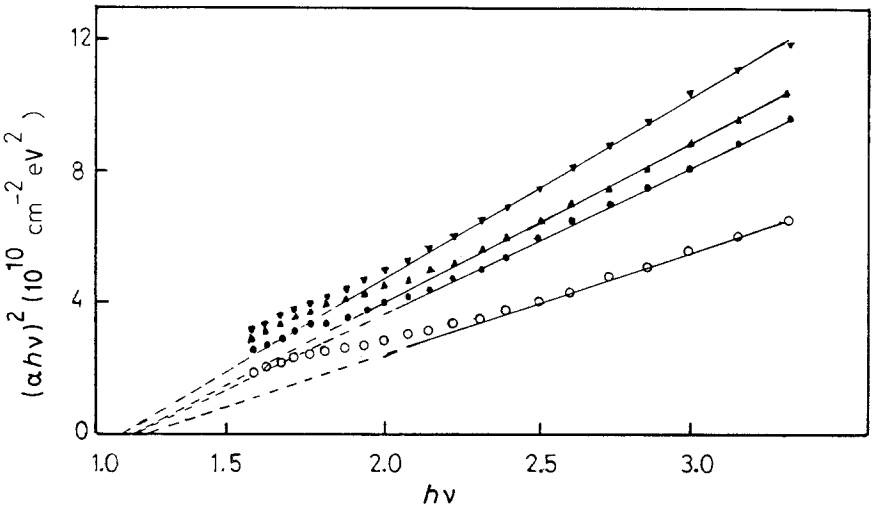

Figure 6 $(\alpha h\nu)^2$ versus $h\nu$ for films annealed at T_a (°C) = (▼) 200, (●) 250, (▲) 350 and (○) 400 for 12 min. d = 120 nm.

TABLE I Variation of E_{opt} and B with film thickness d for as-deposited films and with annealing temperature, T_a, for films with thickness d = 120 nm

	E_{opt} (eV)	B (10^5 cm^{-1} eV$^{1/2}$)
d (nm): 80	0.66	1.07
100	1.12	1.38
120	1.18	2.4
150	1.21	1.96
200	1.21	1.39
T_a (°C): RT	1.18	2.4
200	1.17	2.4
250	1.22	2.17
350	1.21	2.27
400	1.25	1.80

of defects and the localized states, and thus the optical gap increases. On the other hand, a nonsequential change of E_{opt} could be observed with T_a. This behaviour may be due to the nonsequential change of intensity of crystallization of Bi_2Te_2Se with annealing temperature (Fig. 4) which results in a nonsequential change of the number of disorders and defects present in the amorphous matrix with T_a. However, the increase in E_{opt} observed as T_a increased from 350 to 400 °C may be partially due to the loss of tellurium atoms [2, 6]. This tellurium loss causes an increase in the carrier concentration and free carrier absorption, thereby increasing the optical gap.

3.3. High-frequency dielectric constant, ε'_∞

Neglecting multiple reflections, the transmittance of a perfectly smooth film deposited on a perfectly smooth substrate is determined by the relation [16, 17]

$$T = (1 - R)^2 \exp(-A)$$
$$= (1 - R)^2 \exp(-\alpha d) \quad (2)$$

where R is the reflectance and d is the film thickness.

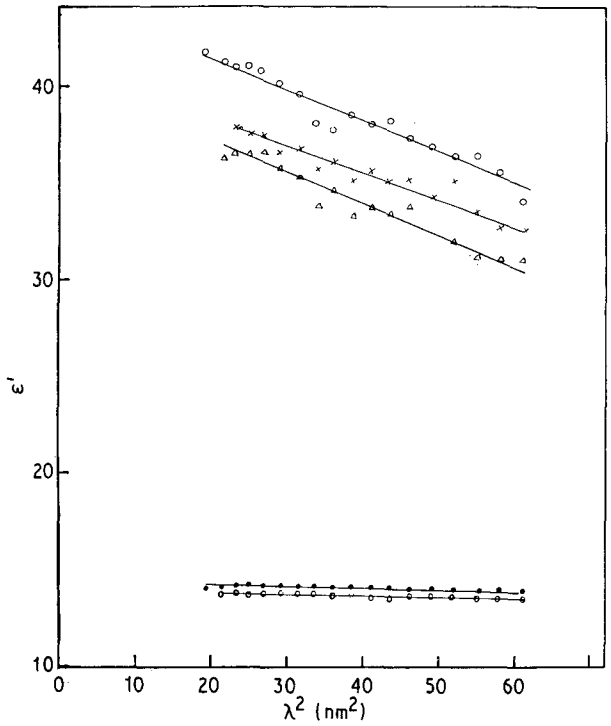

Figure 7 ε′ versus λ^2 for as-deposited Bi_2Te_2Se thin films at d = (○-lower) 80, (●) 100, (×) 120, (○) 150 and (△) 200 nm.

TABLE II Variation of ε'_∞, N/m^* and n_0 with film thickness for as-deposited films and with annealing temperature for films with thickness d = 120 nm

	ε'_∞	N/m^* (10^{22} cm^{-3})	n_0
d(nm): 80	14	0.09	3.5
100	15	0.15	3.7
120	41.1	1.64	6.2
150	46.1	1.78	5.8
200	40.4	1.86	6.0
T_a (°C): RT	41.1	1.64	6.2
200	56	3.12	6.4
250	46	2.23	5.8
350	86	8.36	6.3
400	38	1.54	5.1

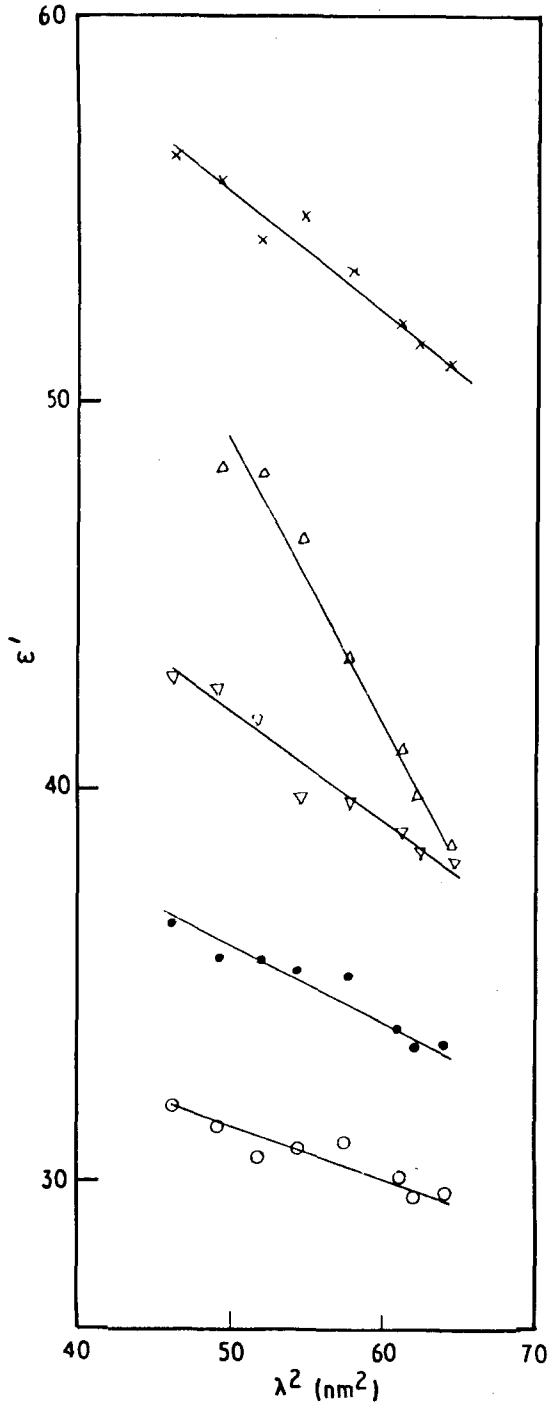

Figure 8 ε′ versus λ^2 for films annealed at T_a (°C) = (▽) 200, (●) 250, (×) 300, (△) 350, (○) 400 for 12 min. d = 120 nm.

Accordingly [18], the real component of the relative permittivity, ε′, and the square of wavelength, λ^2, are correlated through the following equation:

$$\varepsilon' = n^2 = \left(\frac{1 + R^{1/2}}{1 - R^{1/2}}\right)^2 = \varepsilon'_\infty - \frac{e^2}{\pi c^2}\frac{N}{m^*}\lambda^2 \quad (3)$$

where n is the refractive index, ε'_∞ is the infinitely high-frequency dielectric constant, e is the electronic charge, c is the velocity of light and N/m^* is the ratio of carrier concentration to the effective mass. Figs 7 and 8 show the ε′ versus λ^2 plots of the present material at different thicknesses and different temperatures of annealing, respectively. Values of ε'_∞ and n_0 (n_0 is taken as the average value of the refractive index in the range $380 \leqslant \lambda$ (nm) $\leqslant 780$) and N/m^* are shown in Table II.

It is clear that ε'_∞, n_0 and N/m^* are strongly affected by the change in the value of either film thickness or the temperature of annealing. Although, these parameters seem, in general, to increase with film thickness, they change nonsequentially with annealing temperature. On considering the results given in Table II, together with those in Table I and Fig. 4, it can be concluded that the parameters ε'_∞, n_0 and N/m^* are strongly dependent on the internal microstructure change caused by the change in either film thickness or heat treatment.

4. Conclusions

The structure of films prepared by vacuum thermal evaporation at room temperature from melt-quenched Bi_2Te_2Se alloy is partially amorphous. The degree of disordering depends nonsequentially on the temperature of annealing.

The optical parameters E_{opt}, B, ε'_∞, N/m^* and n_0 are affected by both film thickness and annealing temperature. This confirms the effect of these two factors on the density of localized states and microstructure of the test samples.

The spectral dependence of α can be described by Equation 1 with $r = \frac{1}{2}$ in the photon energy range $\sim$ 2–3 eV, indicating direct allowed transitions.

Acknowledgements

The authors thank Professor Dr M. M. Ibrahim for continuous encouragement and stimulating discussions, and Mr H. A. Mahmoud for technical assistance during the optical measurements.

References

1. S. K. MEDHALDHAR and S. P. SENEGUPTA, *Ind. J. Pure Appl. Phys.* **17** (1979) 192.
2. W. BEYER, H. MELL and J. STUKE, *Phys. Status Solidi (b)* **45** (1971) 153.
3. N. TOHGE, T. MINAMI and M. TANAKA, *J. Non-Cryst. Solids* **37** (1980) 23.
4. N. TOHGE, T. MINAMI, Y. YAMAMOTO and M. TANAKA, *J. Appl. Phys.* **51** (1980) 1048.
5. M. SZUKWEI, Y. HANMEI and C. ZONGCAI, *J. Non-Cryst. Solids* **52** (1982) 181.
6. B. D. MURAGI and J. K. ZOPE, *J. Mater. Sci. Lett.* **3** (1984) 663.
7. R. M. MEHRA, P. C. MATHUR, A. K. KATHURIA and R. SHAM, *Phys. Rev. B* **18** (1978) 5620.
8. S. CHAUDHURI, S. K. BISWAS and A. CHOUDHURY, *J. Mat. Sci.* **23** (1988) 4470.
9. M. DI. GIULIO, D. MANNO, R. RELLA, P. SICILIANO and A. TEPORE, *Solar Energy Mater.* **15** (1987) 209.
10. M. M. WAKKAD, *J. Phys. Chem. Solids*, to be published.
11. M. M. IBRAHIM, N. AFIFY, M. M. HAFIZ and M. A. MAHMOUD, *Powder Metall. Int.* **20** (1988) 21.
12. Z. M. DASHEVSKI, T. M. ERUSALIMSKAYA, Ya. A. KALLER, N. V. KOLOMOETS and T. E. SOBOLEVA, *Inorg. Mater.* **13** (1977) 786.
13. F. URBACH, *Phys. Rev.* **92** (1953) 1324.
14. J. TAUC, R. GRIGOROVICI and A. VANCU, *Phys. Status Solidi* **15** (1966) 627.
15. E. A. DAVIS and N. F. MOTT, *Phil. Mag.* **22** (1970) 903.
16. M. BECKER and H. Y. FAN, *Phys. Rev.* **76** (1949) 1530.
17. T. S. MOSS, "Optical Properties of Semiconductors" (Academic Press, New York, 1959) p. 40.
18. W. G. SPITZER and H. Y. FAN, *Phys. Rev.* **106** (1957) 882.

Received 7 November 1990
and accepted 10 April 1991